



Bioinspired Universal Flexible Elastomer-Based Microchannels

Citation

Wu, Feng, Songyue Chen, Baiyi Chen, Miao Wang, Lingli Min, Jack Alvarenga, Jie Ju, et al. 2018. "Bioinspired Universal Flexible Elastomer-Based Microchannels." *Small* 14 (18) (January 11): 1702170. doi:10.1002/smll.201702170.

Published Version

doi:10.1002/smll.201702170

Permanent link

<http://nrs.harvard.edu/urn-3:HUL.InstRepos:37235081>

Terms of Use

This article was downloaded from Harvard University's DASH repository, and is made available under the terms and conditions applicable to Open Access Policy Articles, as set forth at <http://nrs.harvard.edu/urn-3:HUL.InstRepos:dash.current.terms-of-use#OAP>

Share Your Story

The Harvard community has made this article openly available.
Please share how this access benefits you. [Submit a story](#).

[Accessibility](#)

DOI: 10.1002/((please add manuscript number))

Article type: Communication

Bioinspired Universal Flexible Elastomer-Based Microchannels

*Feng Wu, Songyue Chen, Baiyi Chen, Miao Wang, Lingli Min, Jack Alvarenga, Jie Ju, Ali Khademhosseini, Yuxing Yao, Yu Shrike Zhang, Joanna Aizenberg, and Xu Hou**

F. Wu, Dr. M. Wang, Prof. X. Hou

Bionic and Soft Matter Research Institute, College of Physical Science and Technology

Xiamen University

361005, Xiamen, China

E-mail: houx@xmu.edu.cn

Prof. S. Chen

Department of Mechanical and Electrical Engineering

Xiamen University

361005, Xiamen, China

Dr. B. Chen, Dr. L. Min, Prof. X. Hou

College of Chemistry and Chemical Engineering, and Collaborative Innovation Center of Chemistry for Energy

Materials, and State Key Laboratory of Physical Chemistry of Solid Surfaces, and Pen-Tung Sah Institute of Micro-

Nano Science and Technology

Xiamen University

361005, Xiamen, China

Dr. J. Alvarenga, Dr. Y. S. Zhang, Prof. A. Khademhosseini, Prof. J. Aizenberg

Wyss Institute for Biologically Inspired Engineering

Harvard University

MA 02138, Cambridge, USA

Dr. J. Ju, Dr. Y. S. Zhang, Prof. A. Khademhosseini

Biomaterials Innovation Research Center, Division of Engineering in Medicine, Department of Medicine, Brigham

and Women's Hospital

Harvard Medical School

MA 02139, Cambridge, USA

Y. Yao, Prof. J. Aizenberg

Department of Chemistry & Chemical Biology

Harvard University

MA 02138, Cambridge, USA

1 Flexible and stretchable microscale fluidic devices have a broad range of potential
2 applications, ranging from electronic wearable devices for convenient digital lifestyle to
3 biomedical devices. However, simple ways to achieve stable flexible and stretchable fluidic
4 microchannels with dynamic liquid transport have been challenging because every
5 application for elastomeric microchannels is restricted by their complex fabrication
6 process and limited material selection. Here we show a universal strategy for building
7 microfluidic devices that possess exceptionally stable and stretching properties. The
8 devices exhibit superior mechanical deformability, including high strain (967%) and
9 recovery ability, where applications as both strain sensor and pressure-flow regulating
10 device are demonstrated. Various microchannels are combined with organic, inorganic,
11 and metallic materials as stable composite microfluidics. Furthermore, with surface
12 chemical modification these stretchable microfluidic devices can also obtain anti-fouling
13 property to suit for a broad range of industrial and biomedical applications.

14 **Keywords:** Bioinspired, Flexible, Elastomer, Microchannels

1. Introduction

Advances in microfluidics are revolutionizing many traditional disciplines, such as materials science,^[1-4] molecular biology,^[5-7] cellular biology,^[8-12] drug screening,^[3, 13-17] and medical diagnostics.^[18] Elastomeric microfluidics with rapid development in recent years has shown exciting potential from wearable electronic devices^[19-22] for convenient digital lifestyle to biomedical devices^[22-24] that make conformal interfaces with the skin and internal organs. However their broad applications have been significantly restricted by the complex fabrication process^[25, 26] and the limited material selection.^[27-29] For example, Ziegler et al. showed a classic and reproducible method to realize the fabrication of elastomeric microfluidics by micro-molding and thermal bonding of Parylene.^[28] Compared to the general fabrication method, where a sacrificial photoresist layer is sandwiched between two Parylene layers, the poisonous and high-residue photoresist dissolution step is omitted, and the adhesion between the elastomeric Parylene layers is improved. Nevertheless, the micro-molding technique is complicated and expensive, which is difficult to adapt to industry requirements at present. In addition, Ota et al. developed a platform to conveniently fabricate liquid-liquid ‘heterojunction’ devices for the use as liquid-state electronic elastomeric systems.^[27] But this method has been significantly limited by its circumscribed material selection. Moreover, the inner surface of these microchannels are easily contaminated due to the strong adsorption of molecules onto these bulk materials.^[30, 31] The above-

1 mentioned issues have largely affected the development of the conventional elastomeric
2 microfluidic devices and their applications in various fields, such as wearable electronic
3 devices,^[1, 19-22] biomolecule separation,^[32, 33] and anti-fouling technology.^[30, 31]

4 To overcome above challenges, various strategies have been proposed to prepare
5 elastomeric microchannel (EM). Yuk et al. reported a method to assemble hydrogels
6 and elastomers into hybrids with robust interface and functional microstructures, such
7 as microchannels and electrical circuits inside hydrogels.^[34] They used the double-sided
8 acrylic tape elastomers which are made of mixtures of aliphatic acrylate photocured
9 during the film processing (3M VHB membranes) as the good packaging material to
10 seal the hydrogel. Besides, Kubo et al. described a strategy for fabricating the
11 stretchable and mechanically stable radiofrequency antenna, which consisted of liquid
12 metal enclosed in the elastomeric microfluidic channels.^[35] Its high stretchability
13 allowed its resonance to be mechanically tuned over a wide range of frequencies. To
14 date, most of the elastomeric microfluidics works under the conditions of the liquid is
15 enclosed inside the channels without the flowing. Building elastomeric microfluidics
16 with controllable channel sizes and dynamic flowing is still challenging due to material
17 selection limitation, lack of simple and general fabrication process, and fouling issue,
18 but has a great potential applications, such as soft robotics^[36] and tissue engineering.^[37]

19 To address above issues, here we report a universal strategy to build bioinspired
20 flexible elastomer-based microchannel systems with controllable channel sizes, which

show extraordinarily stable and stretchable properties for many potential applications such as the strain sensor and the pressure-flow regulating device. Though showing the excellent flexibility and high adhesion, 3M VHB membrane has been applied in the large research and industrial communities only as the adhesive tapes. Here we used 3M VHB membranes, not only as the good packaging material, but also as the important substrate for directly preparing the microchannels. And our microchannel fabrication is compatible with many existing techniques, such as laser cutting,^[38] blade cutting,^[39] photolithography,^[40] and thermo-molding,^[41] and is also easily scalable for the large-scale fabrication. These stable elastomer-based microchannels not only exhibit excellent flexible and stretchable characteristics, but also can show the good anti-fouling property by further chemical modification of the inner surface of the channels. Such an universal approach for making dynamic microfluidics can potentially serve as a new platform with broad applications.^[1]

2. Results and discussion

2.1. Multi-dimensional microchannels with controllable sizes

Blood vessels in living organisms have multi-dimensional channels structures, with flexibility and stretchability.^[42, 43] Inspired by blood vessels, the multi-dimensional (1D, 2D and 3D) microchannels were fabricated to show the flexible and stretchable properties (**Figure 1a**). For 1D, the EM possessed excellent flexibility, and allowed the

liquid flow inside the channel without any leakage even in a large-scale curve. For 2D, the EM patterned in alphabetic letters would be easily prepared by utilizing the laser cutting method (Figure 1a bottom left and Figure S1, Supporting Information). These microchannels could be homogeneously fabricated, with size easily tuned by the laser power and the engraving time (Table S1 and Figure S2, S3, Supporting Information). For 3D, the elastomer-based microchannels could be obtained by the stacking method, and tested with the external force applied. It showed the excellent sealability after stretching and releasing (Figure 1a bottom right and Video S1, Supporting Information). The size of blood vessels in living organisms are controllable by blood pressure to maintain normal metabolism.^[44, 45] Our bioinspired microchannels could also regulate the channel size by controlling the flow pressure (Figure 1b).

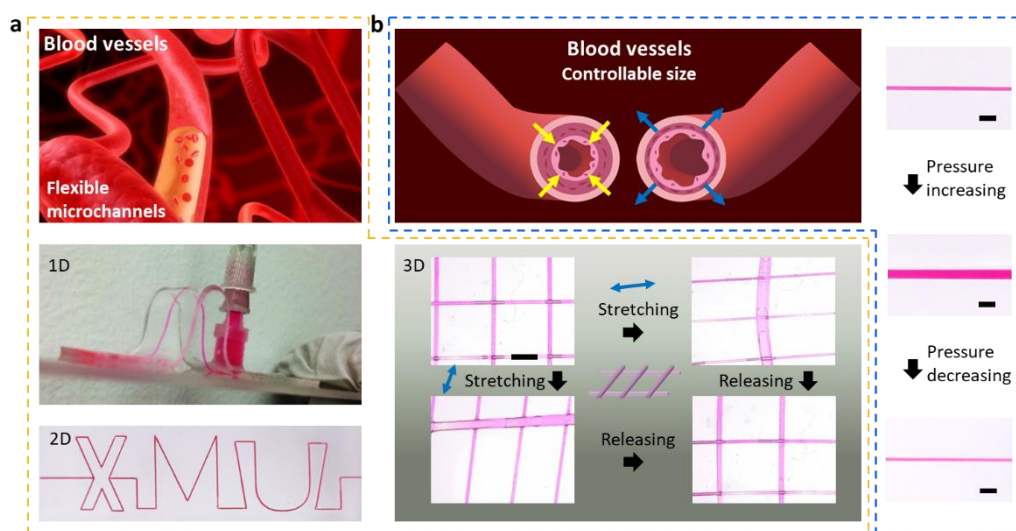


Figure 1. a) Bioinspired flexible microchannels. Flexible blood vessels (Top left). 1D flexible elastomer-based microchannel (Middle left), 2D elastomer-based microchannel with the letter

1 pattern (Bottom left), and 3D elastomer-based microchannels with stretchable and reversible
2 properties (Bottom right). b) Bioinspired microchannels with controllable sizes. Blood vessels with
3 tunable sizes (Top left). The size changes of the elastomer-based microchannel by regulating the
4 flowing pressure (Right). Scale bars, 2 mm.

5 **2.2. Tensile property**

6 One particularity of elastomer-based microchannels originates from its super-elastic
7 property. To further explore the mechanical property, tensile test was performed in
8 comparison with the standard polydimethylsiloxane (PDMS) microchannel, as shown
9 in **Figure 2a**. With the difference from PDMS, the EM sustained continuous spreading
10 and demonstrated the superior stretchability, as well as the elastic-strain recovery ability
11 after releasing (Video S2, Supporting Information). The stress-strain curves of both
12 materials are shown in Figure 2b. The elongation of the EM at break reached $967 \pm$
13 40% , compared with $368 \pm 31\%$ for that of PDMS. The Young's modulus of the EM
14 calculated at linear deformation region reaches ~ 60 kPa, which is a rather low value
15 even for the elastic polymer materials.

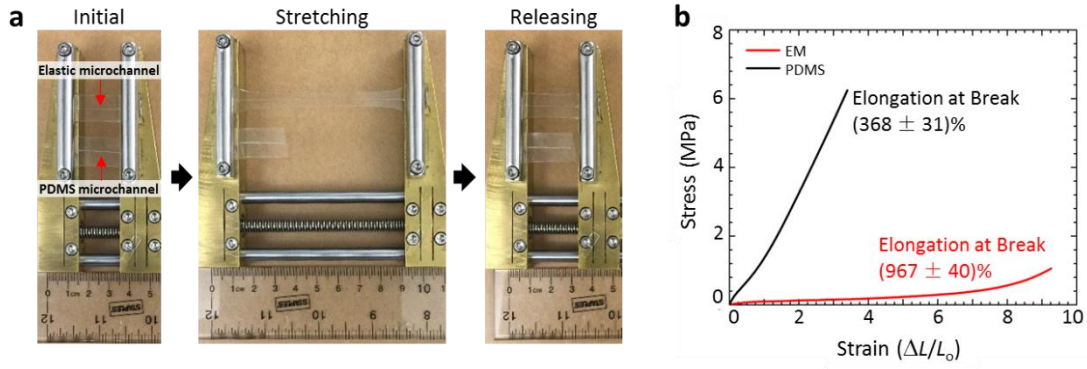


Figure 2. The mechanical property of the elastomeric stretchable microchannel. a) Comparative experiment between the EM and PDMS-based microchannel. b) Stress-strain curves of the EM and PDMS.

2.3. Application as a strain sensor

A strain gauge was designed for the sensitive force sensing based on the outstanding mechanical property of the EM at small forces, as shown in **Figure 3a**. Resistance change of microchannel was measured under different tension. The microchannel was filled with 0.1 M KCl as the ionic conductor, and the current was measured by applying 0.1 V to two Ag/AgCl electrodes inserted into both the inlet and outlet. The ionic conductor in this microchannel served as the deformable interconnections without the risk of cracking as is the concern for metal interconnections.^[46, 47] The normalized resistance change $\Delta R/R$ is a function of strain s :

$$\frac{\Delta R}{R} = \frac{1+s}{(1-\nu s)^2} - 1,$$

where $s = \Delta L/L_0$, and ν represents the Poisson's ratio for the microchannel. Figure 3b shows the normalized resistance change with respect to stress. The corresponding real-

time current change measurement is shown in Figure S4a. The measured Poisson's ratio of EM took the value of ~ 0.15 , while the fitting curve (Figure 3b inset) with the experimental data of ν for the microchannel was 0.093, indicating that compared with the bulk material, the microchannel has less transversal dimension change when being stretched. The strain gauge possesses a force sensitivity of $6\Delta R/R$ per Newton. Another potential advantage of the EM over PDMS for application in sensing lies in that the gas impermeability of the EM allows long-term chemical stability for the liquid filled inside the channel.^[48, 49]

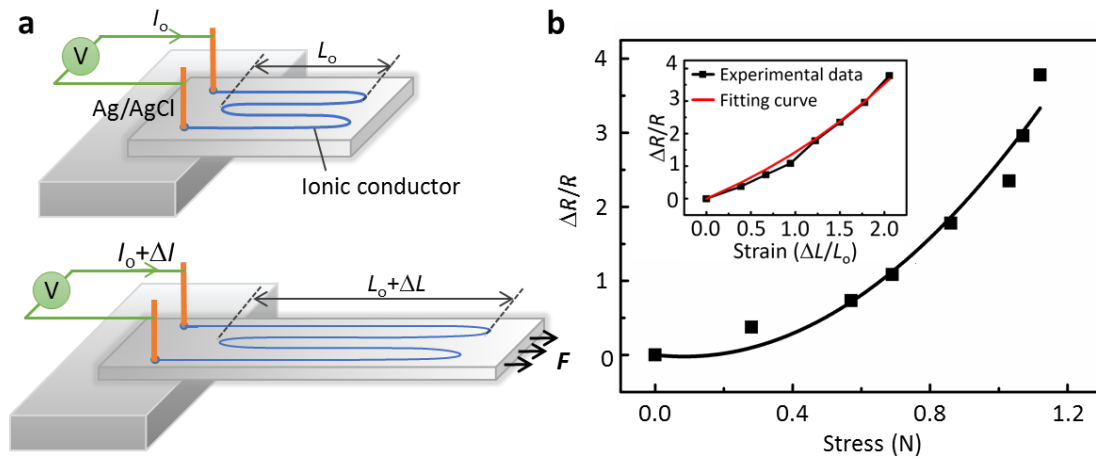


Figure 3. a) Strain gauge based on the EM and the ionic conductor. b) Resistance change curve with the different stress, where the inset is the normalized resistance change with the different strain.

2.4. Lateral deformability

Besides the longitude deformability, the fabricated microchannel device also showed the lateral deformability. The shape of the channel's cross-section was recorded upon stretching the device and releasing. As shown in **Figure 4a**, the six-colored channels of

1 triangular shape were discretely distributed. It should be noted that, there was no liquid
 2 inside the microchannels when we obtained the images of the cross-section of these
 3 channels. Before we obtained these images, the inner wall of these microchannels had
 4 been dyed with the Rhodamine B solution, and then we dried it to obtain a clear contour
 5 of the channels when taking the images during its deformation. By applying an in-plane
 6 force perpendicular to the channels, the initial triangular channels completely closed
 7 and the section thickness decreased. After releasing the force, this highly compressed
 8 state completely recovered and the channels opened again owing to the excellent
 9 elastic property of EM.

10 The force-sensitive deforming feature of this elastomer-based microfluidic device
 11 showed great potential in the application of force/pressure regulation. Figure 4b has
 12 provided a simple illustration of such application. A syringe pump was used here to
 13 supply continuous fluid at a constant flow rate Q ($300 \mu\text{L min}^{-1}$) into a single-channeled
 14 microfluidic device and a digital cantilever capable of supplying small amount of force
 15 was harnessed to exert force to the upper surface of the microchannel. A highly sensitive
 16 pressure gauge connected near the inlet and outlet of the channel was used to monitor
 17 the real-time pressure change. The pressure drop $\Delta P = Q \cdot R_{hyd}$, where flow rate $Q \approx$
 18 $v_s \cdot w \cdot h$, the hydraulic resistance $R_{hyd} \approx \alpha \mu L / wh^3$, and v_s denotes the fluid velocity, μ the
 19 viscosity of the fluid, L , w , and h the length, width and height of the channel for the
 20 rectangular cross-section, respectively, and α the constant related to the shape of the

1 cross-section.^[50, 51] Therefore, for the constant flow rate in our case, ΔP is inversely
2 proportional to h^2 . The cross-section size reduced by pressing on the microchannel,
3 causing the increase of the hydraulic resistance and finally pressure boosting.

4 Specific to the experiment, the initial size of the channel without any pressure was
5 $\sim 250\ \mu\text{m}$ in width, and $\sim 400\ \mu\text{m}$ in height and the velocity of water was set to be $300\ \mu\text{L min}^{-1}$. In the first 200 s, the pressure was building up to a relatively stable value of
6 $13\ \text{kPa}$ without external force to the upper surface. At 400 s, the force of $0.2\ \text{N}$ was
7 exerted to the exterior surface of the channel, ΔP increased accordingly and stabilized
8 at about $11.3\ \text{kPa}$ at 600 s. After that, the force was elevated to $0.6\ \text{N}$, and ΔP underwent
9 another climbing to $18\ \text{kPa}$ at 1000 s. For a microfluidic system with fixed diameter
10 and inner fluid velocity, the force can be detected by using the force-pressure drop
11 calibration curve, indicating a potential application for the pressure sensor system.
12

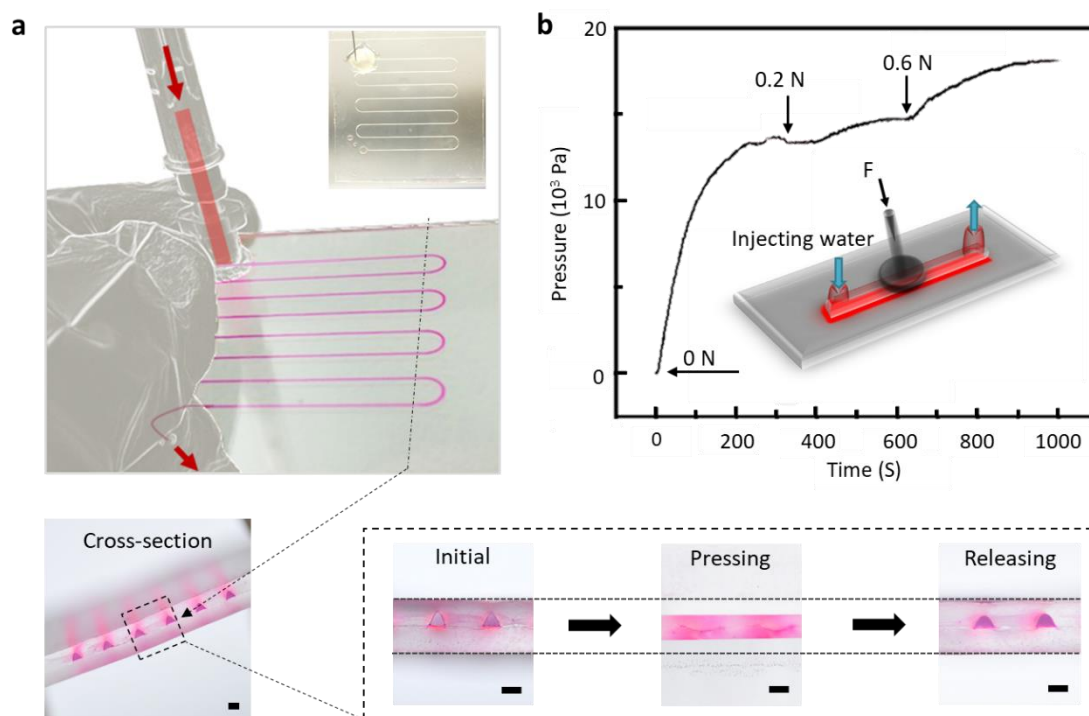
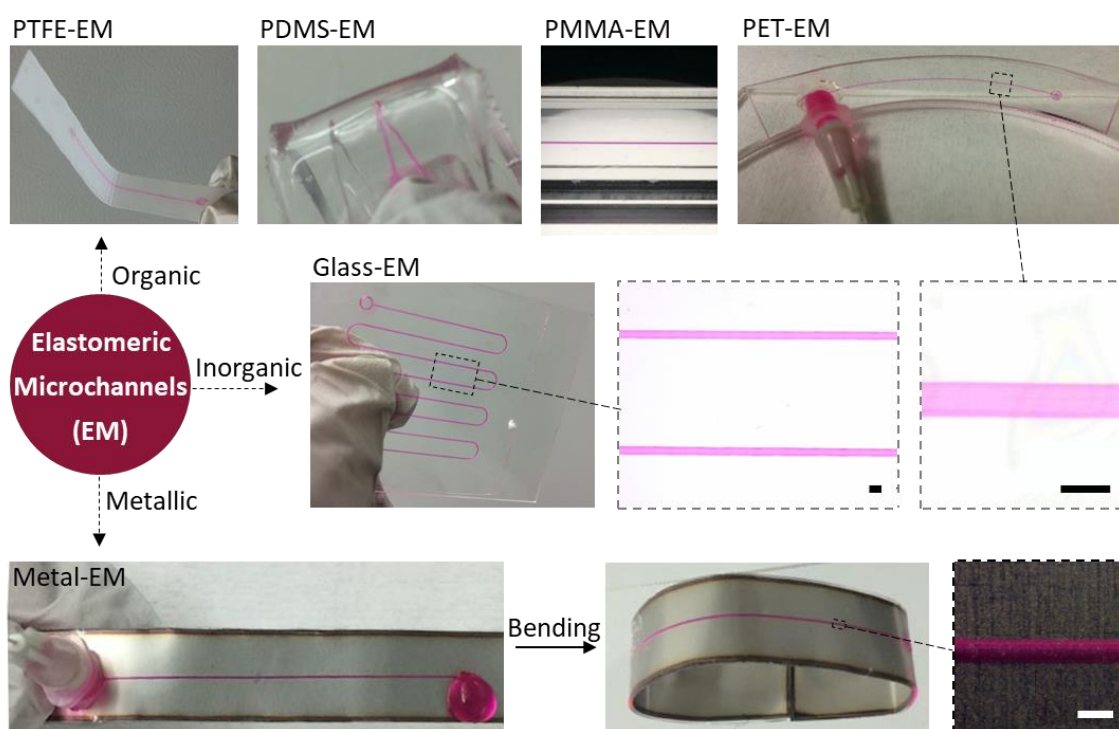


Figure 4. The elastomer-based microchannel's application as a pressure sensor. a) The compressible microchannels and its excellent recovery property. After crosscutting, separated microchannels can be observed clearly. By applying a force perpendicular to the channels, the initial triangular microchannels completely closed and the section thickness decreased. After releasing, the closed microchannels fully recovered again. Inset image shows a clear microfluidics before injection. b) Applied forces can be reflected by the variation of the transfer liquid pressure inside the microchannel. Scale bars, 400 μm .

2.5. Adhesion to various materials

Another superiority of this microfluidics was its vast applicability on various substrates directly, without any surface modifications. As illustrated in **Figure 5**, due to its intrinsic adhesive property, the EM could be transferred on various substrates, including

1 organic (polyethylene terephthalate (PET), polytetrafluoroethylene (PTFE), PDMS,
 2 and polymethyl methacrylate (PMMA)), inorganic (glass), and metallic materials. The
 3 EM adhered firmly onto different types of substrates, and did not show any leakage
 4 from the magnified images. For the metal EM, the seal of the channel was intact even
 5 after severe bending. The 90°-peeling test and the liquid-leakage critical pressure
 6 measurement also showed good sealing property (Figure S5, Supporting Information).



7 **Figure 5.** The composite microfluidics prepared by combining the EM with the organic polymeric
 8 substrates, the inorganic glass substrate, and the metallic substrate. Scale bars, 200 μm.

10 2.6. Surface modification for anti-fouling

11 Fouling is a daunting issue^[30] and restricts practical applications of microfluidic
 12 channels. To avoid fouling, we modified the inner surface of the microchannel with the

1 amphiphobic agent 1H,1H,2H,2H-Perfluorodecyltrimethoxysilane (PFTS) by using the
2 chemical vapor deposition method. As can be observed in **Figure 6**, the evident changes
3 in the wettability and the anti-fouling capacity of the EM occurred in the process of
4 modification. In Figure 6a, water and dimethylsilicone oil were tested as representative
5 chemicals, where the contact angle analysis was used to test the modification. The inner
6 surface of the microchannel without any treatment showed the contact angles of 82.3°
7 to water droplet and 9.7° to dimethylsilicone oil, respectively, indicating an
8 amphipathicity of the EM. However, after modification by PFTS, the remarkable
9 changes took place in the wettability of the EM surface. As shown in Figure 6a, the
10 intrinsic hydrophilicity transformed into hydrophobic (the contact angle of water
11 increased from 82.3° to 118.8°) and the contact angle of dimethylsilicone oil
12 significantly increased from 9.7° to 72.2° . Meanwhile, the PFTS coating exhibited an
13 excellent anti-fouling capacity. As shown in Figure 6b, the modified microchannel inner
14 surface could completely recover to its initial state without any residue of Rhodamine
15 B, while the microchannel without modification showed the serious contamination with
16 the dye molecules. It should be noted that, the surface could also be modified with many
17 other different method to suite different applications, such as the liquid phase
18 deposition^[52] and the chemical composition.^[53]

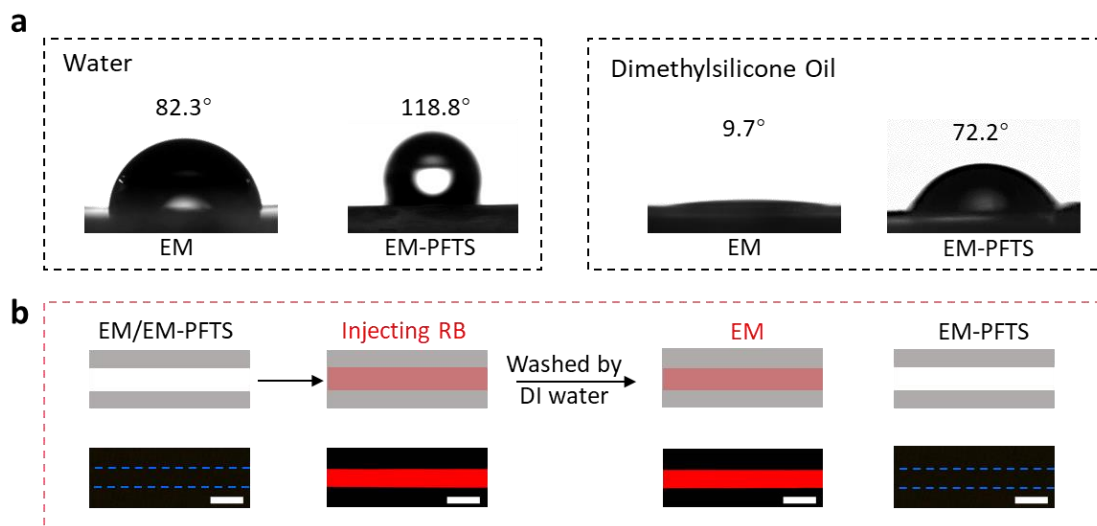


Figure 6. Surface modification of the microchannel inner surface for anti-fouling. a) Water and dimethylsilicone oil contact angle analysis. b) Schematic illustrations (top) and microscopic images of microchannels (bottom). Anti-fouling measurement before and after the surface modification with PFTS on the microchannel inner surface. Scale bars, 50 μm.

3. Conclusion

In summary, we have demonstrated a convenient method to fabricate the elastomer-based microchannel, which possesses the excellent elastic property and dynamic stability with maintaining liquid flows during the stretching and releasing state. Meanwhile, the flexible microchannel can be directly assembled onto various substrates, including organic, inorganic, and metallic. Besides, its inner surface can be conveniently modified by a simple chemical vapor deposition method for anti-fouling application. In addition, the elastomer-based microchannel exhibits excellent mechanical deformability upon stretching (967%) and compressing. Meanwhile, its sensitive deformability upon micro-forces, including both in longitude and lateral

directions, shows great potential in the application for strain sensors and pressure sensors.

4. Experimental Section.

For the microchannels materials, the elastomer (VHB 4910, 3M Company) and PDMS (Sylgard 184, Dow Corning Corporation) with the ratio of base: crosslinker 10: 1 were used. To prevent fouling, PTFE (J&K Chemicals, 227930) was used to modify the microchannel inner surface. Both the deionized water (resistivity 18.3 M Ω cm) and the dimethylsilicone oil (Macklin, D806810) were used to characterize the wetting behavior of the material surface. KCl (Sinopharm, 10016308) was used to act as the ionic conductor. For the anti-fouling measurement, Rhodamine B (Sigma-Aldrich R6626) was used.

Fabrication of microchannels: The flexible and PDMS microchannel were fabricated by cutting the channel directly with versalaser cutting engraving system (GCC, Spirit SI-25), at the power of 50 W and cutting speed of 10 mm s⁻¹. The resolution of this system is 1500 PPI. The flexible 3D microchannels had two layers. We made structures both inside the two layers of the VHB tapes, then adhered them together to fabricate 3D microchannels as shown in Figure 1a.

Mechanical testing: The EM and PDMS microchannels maintained consistent properties over the time of the tests. All microfluidic devices were prepared with 1.5 cm in width, 2.5 cm in length and 2 mm in thickness. The size of channels was \sim 250 μ m

1 in width, and $\sim 400\ \mu\text{m}$ in height. A homemade device was used to test the stretching
2 ability of both EM and PDMS elastomers as shown in Figure 2. Screw tightened bars
3 were utilized to stabilize both ends of samples. Constant tension of the sample could be
4 finely controlled by the device. All tests were performed in ambient air at room
5 temperature.

6 Strain gauge: After we prepared the flexible microchannel pattern with 2 cm in length,
7 1.5 cm in width, and 2 mm in thickness following the abovementioned method, the
8 microchannel was filled with 0.1 M KCl as the ionic conductor. The current was
9 measured while inserting two Ag/AgCl electrodes into the inlet and outlet of the clip. A
10 voltage of 0.1 V was applied by Keithley 2400 source meter. The sensing test was
11 performed by stretching from relaxing length of 2 cm to 5.5 cm.

12 Pressure measurements: A syringe pump was used to supply continuous fluid at a
13 constant flow rate Q ($300\ \text{mL min}^{-1}$) in a single-channeled microfluidics with $\sim 250\ \mu\text{m}$
14 in width, and $\sim 400\ \mu\text{m}$ in height. A digital cantilever capable of supplying small amount
15 of force was harnessed to exert force to the upside surface of the microchannel. A
16 pressure gauge, pressure transmitter (PX273-030DI) from Omega, connected near the
17 inlet and outlet of the channel was used to monitor the real-time pressure change, during
18 flow of deionized water as shown in Figure 4.

19 Peeling test: All substrates were prepared with 2 cm in width, 3 cm in length and 1 mm
20 in thickness. The EM was adhered onto various substrates. The samples were tested

1 with a constant 90°-peeling (Instron 5948 microtester) speed of 10 mm min⁻¹. Steady
2 state of peeling force was finally measured in this process.

3 Liquid-leakage critical pressure measurement: The critical pressure was measured
4 following the method mentioned in the pressure measurements section. The size of
5 channels was ~270 μm in width, and ~500 μm in height.

6 Contact angle measurements: The contact angle was measured with a contact angle
7 measurement system (OCA100, Dataphysics) at room temperature. A droplet of 5 μL,
8 either water or dimethylsilicone oil, was placed on the surface of the sample and the
9 droplet profile was captured. For each sample, a mean value of the contact angle was
10 calculated from at least three individual measurements taken at different locations on
11 the examined samples.

12 Surface modification for anti-fouling: The microchannel was modified by PFTS to
13 obtain the anti-fouling capacity. The size of channels is ~250 μm in width, and ~400
14 μm in height. The exposed microchannel inner surface without any treatment was
15 placed in a desiccator together with an open glass dish containing about 0.5 mL of PFTS.

16 Subsequently, the desiccator was closed again and chemical vapor deposition of silane
17 was carried out for 3 h under 80°C. The inner surfaces finally achieved the anti-fouling
18 capacity, and then the two pieces of modified the EM were adhered to form the
19 microfluidic channel. For comparison, an unmodified microfluidic device was also
20 prepared, and these two microfluidic devices were both injected with the Rhodamine B

aqueous solution. The Rhodamine B aqueous solution used in the microfluidic experiments was prepared by dissolving Rhodamine B in DI water to give a final concentration of 0.1 mg mL⁻¹. After injecting the Rhodamine B solution into the unmodified/modified microfluidic for 5 second, DI water was injected to wash the channels for 30 seconds. During this process, optical microscopy (Leica, DM6000B) was used to observed the fluorescence.

Supporting Information

Supporting Information is available from the Wiley Online Library or from the author.

Acknowledgements

This work is supported by the National Natural Science Foundation of China (No. 21673197), Young Overseas High-level Talents Introduction Plan, the 111 Project (No. B16029), the Fundamental Research Funds for the Central Universities of China (No. 20720170050). J. Aizenberg acknowledges the Department of Energy under Award Number DE-SC0005247 and the Advanced Research Projects Agency-Energy (ARPA-E), U.S. Department of Energy, under Award Number DE-AR0000326. Y. S. Zhang acknowledges the National Cancer Institute of the National Institutes of Health Pathway to Independence Award (K99CA201603), the Lush Prize, and the Science and Technology Commission of Shanghai Municipality (STCSM) 17JC 1400200. The

authors thank M. Eggersdorfer, H. Meng, and Y. Fan for discussion and help. F. Wu, S.

Chen, and B. Chen contributed equally to this work.

Conflict of Interest

The authors declare no conflict of interest.

References

- [1] X. Hou, Y. S. Zhang, G. Trujillo-de Santiago, M. M. Alvarez, J. Ribas, S. J. Jonas, P. S. Weiss, A. M. Andrews, J. Aizenberg, A. Khademhosseini, *Nature Reviews Materials* **2017**, 2, 17016.
- [2] E. K. Sackmann, A. L. Fulton, D. J. Beebe, *Nature* **2014**, 507, 181.
- [3] J. Clayton, *Nat. Methods* **2005**, 2, 621.
- [4] D. Psaltis, S. R. Quake, C. Yang, *Nature* **2006**, 442, 381.
- [5] T. A. Duncombe, A. M. Tentori, A. E. Herr, *Nature reviews Molecular Cell Biology* **2015**, 16, 554.
- [6] G. M. Whitesides, *Nature* **2006**, 442, 368.
- [7] Y. Xu, M. Shinomiya, A. Harada, *Adv. Mater.* **2016**, 28, 2209.
- [8] B. Xiong, K. Ren, Y. Shu, Y. Chen, B. Shen, H. Wu, *Adv. Mater.* **2014**, 26, 5525.
- [9] D. Kim, X. Wu, A. T. Young, C. L. Haynes, *Acc. Chem. Res.* **2014**, 47, 1165.
- [10] Y. Cheng, F. Zheng, J. Lu, L. Shang, Z. Xie, Y. Zhao, Y. Chen, Z. Gu, *Adv. Mater.* **2014**, 26, 5184.
- [11] Y. S. Zhang, A. Khademhosseini, *Science* **2017**, 356, 3627.
- [12] S. Cheng, Y. Jin, N. Wang, F. Cao, W. Zhang, W. Bai, W. Zheng, X. Jiang, *Adv. Mater.* **2017**, 29, 1700171.
- [13] S. Xiao, J. R. Coppeta, H. B. Rogers, B. C. Isenberg, J. Zhu, S. A. Olalekan, K. E. McKinnon, D. Dokic, A. S. Rashedi, D. J. Haiseneder, *Nat. Commun.* **2017**, 8, 14584
- [14] R. C. R. Wootton, A. J. Demello, *Nature* **2012**, 483, 43.
- [15] A. Albanese, A. K. Lam, E. A. Sykes, J. V. Rocheleau, W. C. W. Chan, *Nat. Commun.* **2013**, 4, 2718.
- [16] P. M. Valencia, O. C. Farokhzad, R. Karnik, R. Langer, *Nature Nanotech.* **2012**, 7, 623.
- [17] P. Mitchell, *Nat. Biotechnol.* **2001**, 19, 717.

- 1 [18] P. Yager, T. Edwards, E. Fu, K. Helton, K. Nelson, M. R. Tam, B. H. Weigl, *Nature*
2 **2006**, *442*, 412.
- 3 [19] M. Kaltenbrunner, T. Sekitani, J. Reeder, T. Yokota, K. Kuribara, T. Tokuhara, M.
4 Drack, R. Schwödiauer, I. Graz, S. Bauer-Gogonea, *Nature* **2013**, *499*, 458.
- 5 [20] S. Xu, Y. Zhang, L. Jia, K. E. Mathewson, K. I. Jang, J. Kim, H. Fu, X. Huang, P.
6 Chava, R. Wang, *Science* **2014**, *344*, 70.
- 7 [21] J. C. Yeo, J. Yu, K. P. Loh, Z. Wang, C. T. Lim, *ACS Sensors* **2016**, *1*, 543.
- 8 [22] X. Pu, M. Liu, X. Chen, J. Sun, C. Du, Y. Zhang, J. Zhai, W. Hu, Z. Wang, *Sci.*
9 *Adv.*, **2017**, *3*, e1700015.
- 10 [23] A. Chortos, J. Liu, Z. Bao, *Nature Mater.* **2016**, *15*, 937.
- 11 [24] J. Kim, M. Lee, H. J. Shim, R. Ghaffari, H. R. Cho, D. Son, Y. H. Jung, S. Min,
12 C. Choi, S. Jung, *Nat. Commun.* **2014**, *5*, 5747.
- 13 [25] D. Qin, Y. Xia, G. M. Whitesides, *Nat. Protoc.* **2010**, *5*, 491.
- 14 [26] M. K. Verma, A. Majumder, A. Ghatak, *Langmuir*. **2006**, *22*, 10291.
- 15 [27] H. Ota, K. Chen, Y. Lin, D. Kiriya, H. Shiraki, Z. Yu, T. J. Ha, A. Javey, *Nat.*
16 *Commun.* **2014**, *5*, 5032.
- 17 [28] D. Ziegler, T. Suzuki, S. Takeuchi, *J. Microelectromech. Syst.* **2006**, *15*, 1477.
- 18 [29] S. Metz, R. Holzer, P. Renaud, *Lab on a chip* **2001**, *1*, 29.
- 19 [30] R. Mukhopadhyay, *Anal. Chem.* **2005**, *77*, 429.
- 20 [31] K. J. Regehr, M. Domenech, J. T. Koepsel, K. C. Carver, S. J. Ellison-Zelski, W.
21 L. Murphy, L. A. Schuler, E. T. Alarid, D. J. Beebe, *Lab on a chip* **2009**, *9*, 2132.
- 22 [32] S. Marre, Y. Roig, C. Aymonier, *J. Supercrit. Fluid.* **2012**, *66*, 251.
- 23 [33] N. Kockmann, J. Kastner, P. Woias, *Chem. Eng. J.* **2008**, *135*, S110.
- 24 [34] H. Yuk, Z. Teng, G. A. Parada, X. Liu, X. Zhao, *Nat. Commun.* **2016**, *7*, 12028.
- 25 [35] M. Kubo, X. Li, C. Kim, M. Hashimoto, B. J. Wiley, D. Ham, G. M. Whitesides,
26 *Adv. Mater.* **2010**, *22*, 2749.
- 27 [36] S. A. Morin, G. M. Whitesides, *Science* **2012**, *337*, 828.
- 28 [37] I. Wagner, E. M. Materna, S. Brincker, U. Süssbier, C. Frädrich, M. Busek, F.
29 Sonntag, D. A. Sakharov, E. V. Trushkin, A. G. Tonevitsky, *Lab on a chip* **2013**, *13*,
30 3538.
- 31 [38] D. Snakenborg, H. Klank, J. P. Kutter, J. Micromech. *Microeng.* **2003**, *14*, 182.
- 32 [39] F. Cortés-Salazar, M. Träuble, F. Li, J. M. Busnel, A. L. Gassner, M. Hojeij, G.
33 Wittstock, H. H. Girault, *Anal. Chem.* **2009**, *81*, 6889.
- 34 [40] J. R. Anderson, D. T. Chiu, H. Wu, O. Schueller, G. M. Whitesides,
35 *Electrophoresis* **2000**, *21*, 27.
- 36 [41] K. Ren, W. Dai, J. Zhou, J. Su, H. Wu, *Proc. Natl. Acad. Sci. USA.* **2011**, *108*,
37 8162.
- 38 [42] A. C. Burton, *Am. J. Physiol.* **1951**, *164*, 319.

- [43] W. Wu, A. Deconinck, J. A. Lewis, *Adv. Mater.* **2011**, 23, 178.
- [44] B. Yuan, Y. Jin, Y. Sun, D. Wang, J. Sun, Z. Wang, W. Zhang, X. Jiang, *Adv. Mater.* **2012**, 24, 890.
- [45] P. Gong, W. Zheng, Z. Huang, W. Zhang, D. Xiao, X. Jiang, *Adv. Funct. Mater.* **2013**, 23, 42.
- [46] J. Lee, J. Wu, M. Shi, J. Yoon, S. Park, M. Li, Z. Liu, Y. Huang, J. A. Rogers, *Adv. Mater.* **2011**, 23, 986.
- [47] Y. Su, X. Ping, K. J. Yu, J. W. Lee, J. A. Fan, B. Wang, M. Li, R. Li, D. V. Harburg, Y. Huang, *Adv. Mater.* **2017**, 29, 1604989.
- [48] K. Ren, Y. Chen, H. Wu, *Curr. Opin. Chem. Biol.* **2014**, 25, 78.
- [49] P. L. Floch, X. Yao, Q. Liu, Z. Wang, G. Nian, Y. Sun, L. Jia, Z. Suo, *ACS Appl. Mat. Interfaces*, **2017**, DOI: 10.1021/acsami.7b07361.
- [50] C. J. Morris, F. K. Forster, *Exp. Fluids*. **2004**, 36, 928.
- [51] M. J. Fuerstman, A. Lai, M. E. Thurlow, S. S. Shevkoplyas, H. A. Stone, G. M. Whitesides, *Lab on a chip* **2007**, 7, 1479.
- [52] M. Y. Liu, H. Wang, Y. Wang, *Aiche. J.* **2010**, 53, 1075.
- [53] Andrea R. Statz, Robert J. Meagher, a. Annelise E. Barron, Phillip B. Messersmith, *J. Am. Chem. Soc.* **2005**, 127, 7972.

Supporting Information**Bioinspired Universal Flexible Elastomer-Based Microchannels**

*Feng Wu, Songyue Chen, Baiyi Chen, Miao Wang, Lingli Min, Jack Alvarenga, Jie Ju, Ali Khademhosseini, Yuxing Yao, Yu Shrike Zhang, Joanna Aizenberg, and Xu Hou**

F. Wu, Dr. M. Wang, Prof. X. Hou

Bionic and Soft Matter Research Institute, College of Physical Science and Technology

Xiamen University

361005, Xiamen, China

E-mail: houx@xmu.edu.cn

Prof. S. Chen

Department of Mechanical and Electrical Engineering

Xiamen University

361005, Xiamen, China

Dr. B. Chen, Dr. L. Min, Prof. X. Hou

College of Chemistry and Chemical Engineering, and Collaborative Innovation Center of Chemistry for Energy

Materials, and State Key Laboratory of Physical Chemistry of Solid Surfaces, and Pen-Tung Sah Institute of Micro-

Nano Science and Technology

Xiamen University

361005, Xiamen, China

Dr. J. Alvarenga, Dr. Y. S. Zhang, Prof. A. Khademhosseini, Prof. J. Aizenberg

Wyss Institute for Biologically Inspired Engineering

Harvard University

MA 02138, Cambridge, USA

Dr. J. Ju, Dr. Y. S. Zhang, Prof. A. Khademhosseini

Biomaterials Innovation Research Center, Division of Engineering in Medicine, Department of Medicine, Brigham

and Women's Hospital

Harvard Medical School

MA 02139, Cambridge, USA

Y. Yao, Prof. J. Aizenberg

Department of Chemistry & Chemical Biology

Harvard University

MA 02138, Cambridge, USA

For 3D microchannels (Video S1, Supporting Information), there were discontinuous microchannels that we specially designed to test the sealability of the microfluidics. The discontinuously microchannels would block the liquid flow during stretching and releasing state that showed the excellent sealing.

The channels could be homogeneously fabricated (Figure S1 and S2, Supporting Information). Meanwhile, this method was also applicable for the microchannel sizes down to the sub-micron scale (Figure S2, Supporting Information).

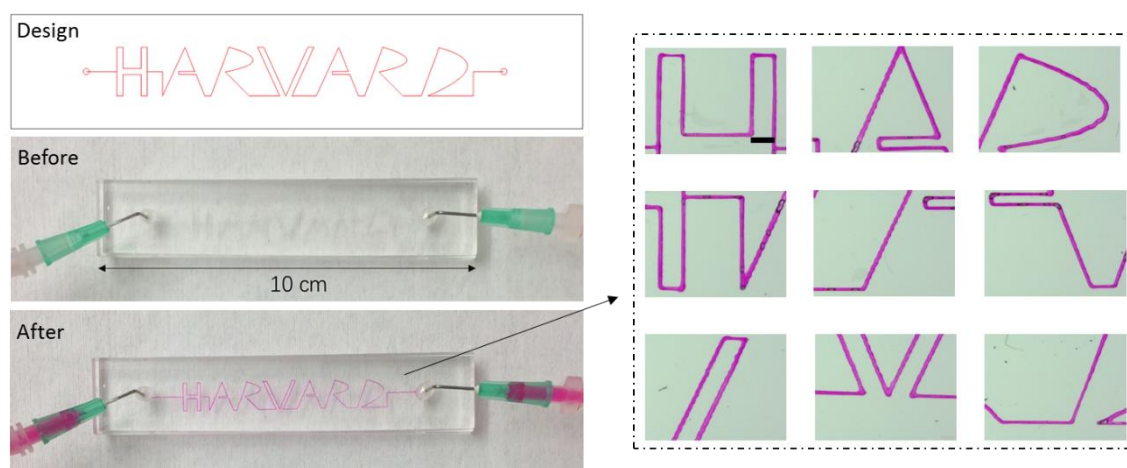


Figure S1. The pattern “HARVARD” of microchannel was designed to prepare the 2D microchannel (Left). More details about the microchannel were shown on the right. Scale bar, 1 mm.

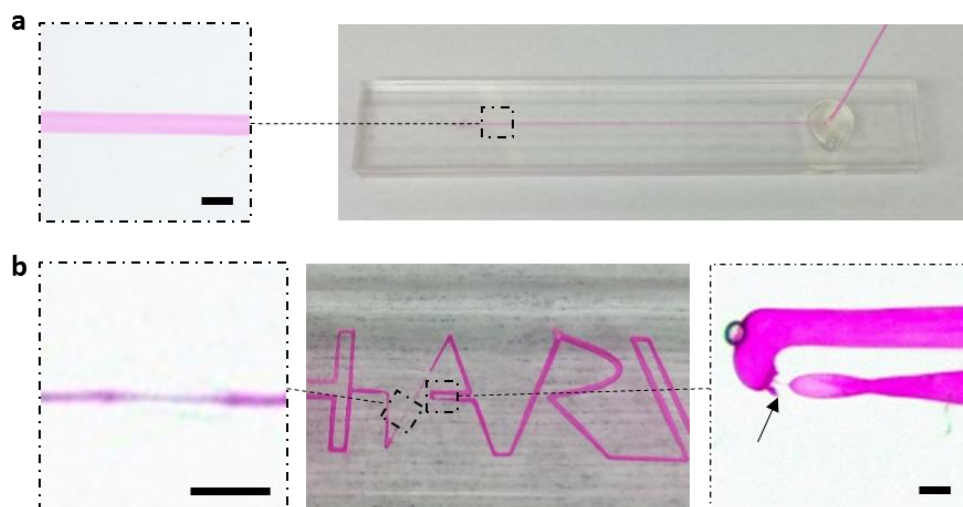


Figure S2. a) The homogeneous microchannel. b) The channel was fabricated with the size of tens of micrometers down to sub-micron. Scale bars, 200 μm .

The channel dimensions could be controlled by the laser power and the engraving time. In this work, we studied the impact of engraving speed on the size of the channels at the power of 50 W. Table S1 and Figure S3 indicate that the lower cutting speeds would increase the channel sizes, while higher cutting power would accumulate on the substrate at a slower speed. It is worth noting that the laser would pass through the EM at speed of less than 3 mm/s. The smallest size of channel fabricated by the laser cutting system was $\sim 200\ \mu\text{m}$ due to the limitation of the spot size of the versalaser cutting system, which was above $70\ \mu\text{m}$.

Table S1. Different sizes of the microchannel prepared at the different engraving speeds.

Engraving speed (mm/s)	20	15	10	7
Height (μm)	151.38	189.17	392.85	510.37
Width (μm)	207.14	224.05	254.58	278.73

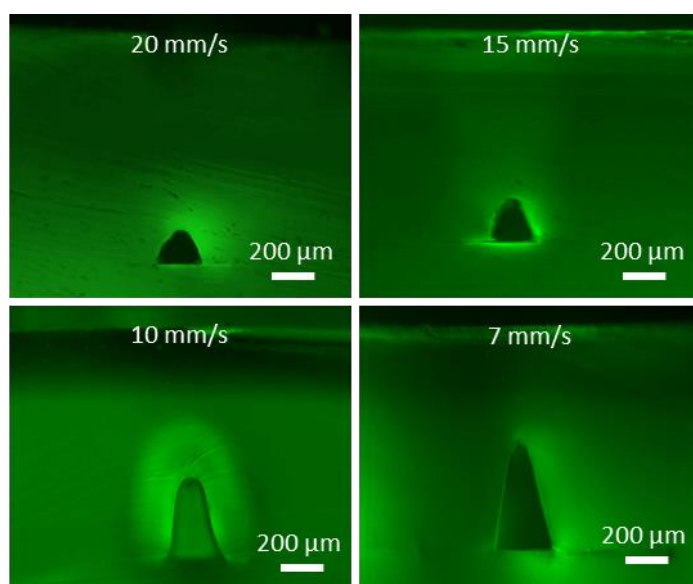


Figure S3. The cross-section of elastomer-based microchannel fabricated at the different engraving speeds.

The force sensor remained stable after being stretched 2 times of the original length for 10 s; then it was released completely and maintains for 15 s.

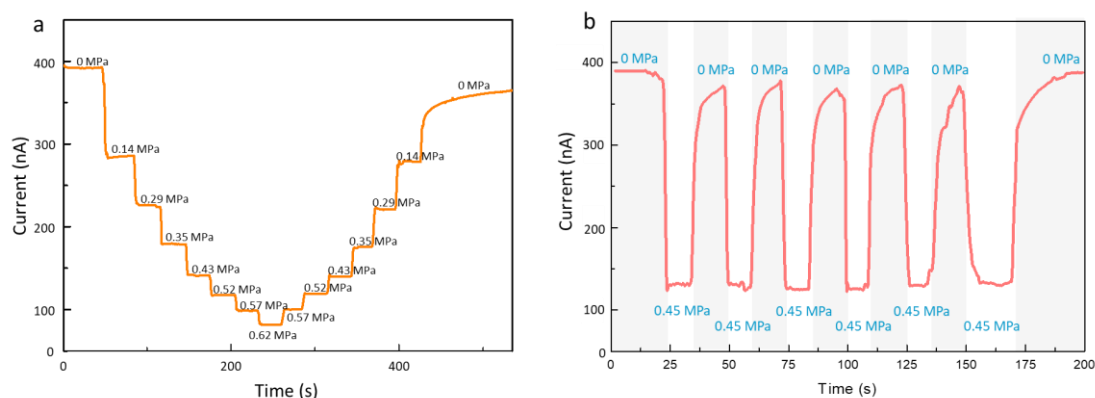
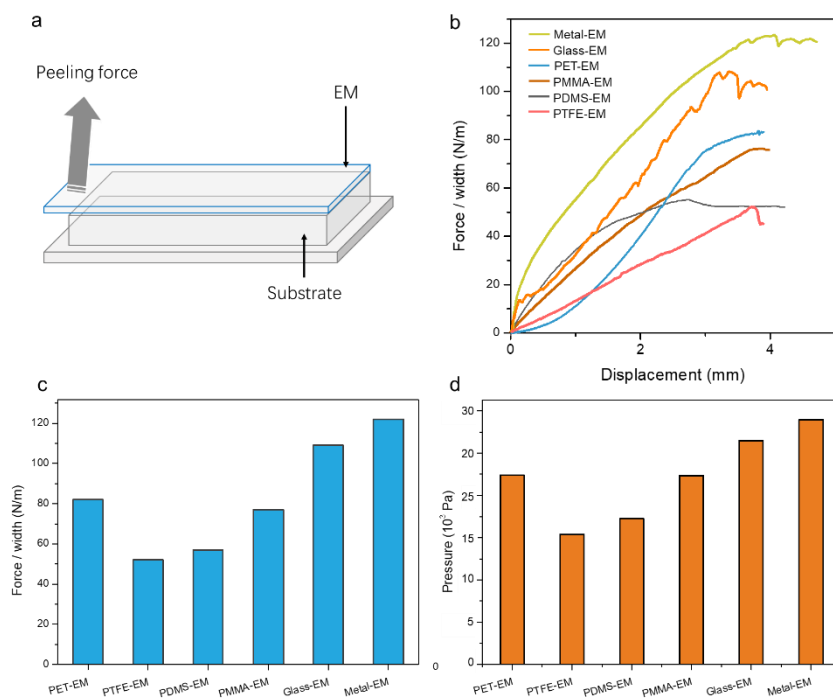


Figure S4. a) The real-time strain gauge testing by stretching and releasing the elastomer-based microchannel. The current was measured with the stretching EM at 0.5 cm per interval. The value of the forces is shown above the curve. b) Current changes under repeated the stretch and release from 0% to 100% for the cycles test.

To measure the adhesion between EM and various substrates, we used the 90°-peeling test and the liquid-leakage critical pressure measurement, as shown in Figure S5. The peeling force (Figure S5a-c, Supporting Information) was consistent with the liquid-leakage critical pressure (Figure S5d, Supporting Information) in the order Metal-EM > Glass-EM > PET-EM > PMMA-EM > PDMS-EM > PTFE-EM. This similarity could be explained by the surface energy or surface roughness. Overall, the liquid-leakage critical pressure was more than the liquid-leakage critical pressure (~3.3 MPa), exhibiting the good sealing property.



1

2 **Figure S5.** a-c) The 90°-peeling test between the EM and various substrates. d) The liquid-leakage critical pressure

3 between the EM and various substrates.